ELSEVIER

Journal of Alloys and Compounds 303–304 (2000) 480–488

Journal of ALLOYS AND COMPOUNDS

www.elsevier.com/locate/jallcom

Magnetic fluctuations in $CeCu_{6-x}Au_x$ at the nonmagnetic–magnetic quantum phase transition

H.v. Löhneysen*, A. Schröder, O. Stockert

Physikalisches Institut, Universität Karlsruhe, D-76128 Karlsruhe, Germany

Abstract

When the heavy-fermion system $CeCu_6$ is doped with Au, long-range antiferromagnetic order develops above a threshold concentration $x = 0.1$, with T_N reaching 2.3 K for $x = 1$. The magnetic ordering vector of $CeCu_{6-x}Au_x$ as determined from elastic neutron scattering is almost independent of x for $x = 0.15$, 0.2 and 0.3, $Q \approx (0.63\ 0\ 0.26)$, and jumps to the a^* axis for $x = 0.5$. At the quantum critical point $x = 0.1$, the specific heat C exhibits a divergence of $C/T \sim -\ln(T/T_0)$ towards low temperatures T, and the electrical resistivity varies linearly with T. Inelastic neutron scattering experiments were carried out at the ILL Grenoble and at Risø in order to investigate whether the critical fluctuations for $x = 0.1$ can account for this anomalous behavior. We review some salient features of the both data sets. The observed reduced dimensionality of the critical fluctuations indeed leads to the above anomalous behavior. A detailed study of the energy and temperature dependence of the dynamic structure factor reveals unusual dynamics. The orthorhombic–monoclinic distortion in $CeCu_6$ is suppressed rapidly with increasing x and is shown to be unrelated to the quantum phase transition.

Keywords: Magnetically ordered materials; Heavy-fermions; Kondo effects phase transitions; Spin dynamics; Neutron scattering; Diffraction

1. Introduction

In heavy-fermion systems (HFS) with (often) a regular sublattice of rare-earth or actinide atoms, notably Ce, Yb, or U, a change of the magnetic behavior occurs with decreasing temperature T from that of a collection of 'free' localized $4f$ or $5f$ magnetic moments (modified by the crystalline electric field) coupled weakly to the conduction electrons, to low-T local singlets where the localized moment — under certain circumstances — is screened completely by the conduction electrons through the Kondo effect. The energy gain of the singlet formation $k_B T_K \sim \exp(-1/N(E_F)J)$ sets the temperature scale where this change occurs. Here $N(E_F)$ is the (unrenormalized) conduction-electron density of states at the Fermi level and J is the conduction-electron $-$ f-electron exchange constant.

At sufficiently low $T \ll T_K$, Fermi-liquid (FL) properties are observed in a number of HFS with, however, a very large effective mass m^* derived from the huge linear specific-heat coefficient $\gamma := C/T$ and a correspondingly large Pauli susceptibility χ, both being only weakly dependent on T. The electrical resistivity of a FL exhibits a contribution $\Delta\rho = AT^2$ arising from particle–particle collisions [1,2]. In HFS the energy scale corresponding to E_F in the free-electron gas is set by the Kondo temperature T_K which is of the order of 10–100 K (sometimes even lower). The phenomenological correlations $\gamma \sim \chi$ [6] and $A \sim \gamma^2$ [7] approximately observed for different HFS do suggest the validity of the FL description. The Wilson ratio $R = (\chi/\gamma)(\pi^2 k_B^2/3\mu_0\mu_{eff}^2)$ deviates from the free-electron value $R = 1$. The observed values of $R \sim 2$–5 can be accounted for in the frame of FL theory [1,2] by a negative Landau parameter F_0^a, i.e., $\gamma = (m^*/m_0)\gamma_0$ and $\chi = (m^*/m_0)\ \chi_0/(1 + F_0^a)$, where γ_0 and χ_0 are the free-electron values.

The competition between on-site Kondo interaction quenching the $4f$ or $5f$ localized magnetic moments and intersite Ruderman–Kittel–Kasuya–Yosida (RKKY) interaction between these moments via the conduction electrons allows for nonmagnetic or magnetically ordered ground-states in HFS. In a simple picture [8], this competition is governed by a single parameter, namely the effective exchange constant J between conduction electrons and local moments, which enters the characteristic energy scales $k_B T_K$ and $k_B T_{RKKY} \sim J^2 N(E_F)$ for Kondo and RKKY interactions, respectively. The strength of the exchange interaction is often tuned by composition or pressure.

*Corresponding author. Tel.: +49-721-608-3441; fax: +49-721-608-6103.

0925-8388/00/$ – see front matter
PII: S0925-8388(00)00631-9

Owing to the extremely strong dependence of the Kondo energy on the interatomic distance d which is reflected in their very large Grüneisen parameter in these materials [9], volume changes are often the dominant effect in producing the magnetic–nonmagnetic transition. In the vicinity of the magnetic–nonmagnetic transition non-Fermi-liquid (NFL) behavior [5] manifests itself as a strong deviation of thermodynamic and transport properties from FL predictions, often $\gamma \sim -\ln(T/T_0)$, and $\Delta\rho \sim T^m$ with $m < 2$.

It is generally believed that the NFL behavior observed in HFS at the magnetic–nonmagnetic transition arises from a proliferation of magnetic excitations [3,4,10]. This transition, being induced by an external parameter such as concentration or pressure, may in principle occur at $T = 0$. If the transition is continuous, it is driven by quantum fluctuations instead of thermal fluctuations in finite-T transitions. The critical behavior of such a quantum-phase transition (QPT) at $T = 0$ is governed by the dimension d and the dynamic exponent z. In the Hertz–Millis theory [3,4] the effective dimension is given by $d_{\rm eff} = d + z$. Hence one is in general above the upper critical dimension $d_{\rm eff} = 4$ except in the marginal case $d = z = 2$.

While in three spatial dimensions the renormalization-group treatment by Millis [4] essentially corroborates the previous predictions of the self-consistent renormalization (SCR) theory of spin fluctuations [10], new results are obtained for two-dimensional (2D) systems. The case of 2D fluctuations coupled to itinerant quasiparticles with 3D dynamics has been worked out by Rosch et al. [11]. This case is pertinent to the unusual situation in $CeCu_{6-x}Au_x$ as will be explained below.

Since many of the HFS are driven through the QPT by changing the composition, thus introducing disorder, its effect on the critical behavior is an important issue. In HFS alloys we have to distinguish disorder by dilution of the 4*f* or 5*f* site as, e.g., in $Ce_{1-x}La_xRu_2Si_2$, and by altering the ligand configuration as, e.g., in $CeCu_{6-x}Au_x$. A priori, it is not clear how the disorder acts in both circumstances. In the first case, a 'Kondo hole' introduced by dilution might lead to substantial scattering and ultimate loss of coherence. In the second case, on the other hand, the Ce atoms experience different local environments and this may lead to different local Kondo temperatures. A broad distribution of T_K may also lead to NFL behavior [12,13].

Recently, Castro Neto et al. considered the possibility that a metallic paramagnetic phase coexists with a granular magnetic phase due to disorder [14]. This is suggested to be analogous to a Griffiths phase of dilute magnetic alloys [15]. Because of the cluster formation in the paramagnetic region, power-law T-dependences of thermodynamic quantities are predicted, i.e., $C/T \sim \chi \sim T^{-1+\lambda}$ with $\lambda < 1$. This model was tested by de Andrade et al. [16] for a number of strongly disordered U alloys exhibiting NFL behavior. The systems analyzed all have electrical resistivities ρ well in excess of 200 $\mu\Omega$ cm at low T and exhibit a negative temperature coefficient $d\rho/dT < 0$ indicating that they are far from a coherent FL even well away from the critical point where magnetic order is observed. The data can indeed well be described by a power-law behavior of $C(T)$ and $\chi(T)$ with λ clustering around 0.7, with significant deviations (up to 0.2) between the C-derived and χ-derived λ values. In elucidating the role of disorder, it is important to distinguish between short-range disorder as in an ideal random solid solution, and long-range disorder as in inhomogeneous alloys with long-range concentration fluctuations or even phase separation.

In this review, we will focus on $CeCu_{6-x}Au_x$ which appears to be one of the best studied examples of NFL behavior and, in addition, presents very unusual spin dynamics as measured with neutron scattering. This paper is organized as follows: Section 2 reviews the thermodynamic properties of $CeCu_{6-x}Au_x$, Section 3 discusses the magnetic order and magnetic fluctuations as observed with elastic and inelastic neutron scattering, and Section 4 addresses the structural aspects of $CeCu_{6-x}Au_x$, viz. the orthorhombic–monoclinic transition occurring for low x. The reader who is interested in more details is referred to Refs. [17,18] for a review of macroscopic non-Fermi-liquid properties, to Ref. [19] for the interplay of magnetic structure and electronic transport and to Ref. [20] for a general review of Fermi-liquid instabilities at the magnetic–nonmagnetic transition and a discussion of other NFL scenarios such as a two-channel Kondo effect or a T_K distribution.

2. Review of thermodynamic and transport properties of $CeCu_{6-x}Au_x$

$CeCu_6$ crystallizes in the orthorhombic Pnma structure and undergoes an orthorhombic–monoclinic phase transition around $T_{om} \approx 220$ K (see Chapter 4). The monoclinic distortion is only small ($\sim 1.5°$). In order to avoid confusion, we use the orthorhombic notation for the direction of the lattice vectors throughout this paper. Pure $CeCu_6$ is a HFS showing no long-range magnetic order down to the range of $\sim$ 20 mK [21,22]. With $\gamma = 1.6$ J/mol K^2 it is one of the 'heaviest' HFS. $CeCu_6$ exhibits a pronounced magnetic anisotropy with the magnetization ratios along the three axes M_c:M_a:$M_b \approx 10$:2:1 at low T [22].

Although $CeCu_6$ does not order magnetically[1] [23,24] it exhibits intersite antiferromagnetic fluctuations as observed with inelastic neutron scattering by peaks in the dynamic structure factor $S(q,\omega)$ for energy transfer $\hbar\omega = 0.3$ meV at $Q = (1\ 0\ 0)$ and $(0\ 1 \pm 0.15\ 0)$ [25]. The rather large widths of these peaks correspond to correlation lengths extending roughly only to the nearest Ce neighbors. These correlations vanish at a field of $\sim$2 T. The breaking of the

[1] We do not consider the possible magnetic ordering (electronic or nuclear) that might occur at a few mK.

antiferromagnetic correlations by a magnetic field (often referred to as metamagnetic transition) has been also observed in the differential magnetic susceptibility dM/dB as a shallow maximum at 2 T at very low T [26].

Upon alloying with Au the $CeCu_6$ lattice expands [27], thus weakening the hybridization between Ce 4*f* electrons and conduction electrons. Hence J decreases leading to a stabilization of localized magnetic moments which can now interact via the RKKY interaction. The result is antiferromagnetic order in $CeCu_{6-x}Au_x$ beyond a threshold concentration $x_c \approx 0.1$, as inferred early from sharp maxima in the specific heat $C(T)$ [28] and magnetization $M(T)$ [28,29]. For $0.1 < x \leq 1$ the Néel temperature T_N varies linearly with x (Fig. 1). For the stoichiometric compound $CeCu_5Au$ a complex magnetic phase diagram has been mapped out [30]. The decrease of $T_N(x)$ beyond $x = 1$ coincides with a subtle change within the orthorhombic structure: for $x < 1$ the lattice parameters a and c increase, while b decreases with growing Au content, whereas for $x > 1$ all three lattice parameters a, b and c increase [27]. For all x up to 1.5, the unit-cell volume increases. The long-range antiferromagnetic order has been confirmed by neutron scattering as will be discussed below.

Fig. 2 shows specific-heat data for concentrations in the vicinity of the critical concentration $x_c \approx 0.1$ plotted as C/T versus log T [31]. The Néel temperature T_N manifests itself as a sharp kink in C/T which becomes less pronounced as T_N decreases. It is, however, still clearly visible for $x = 0.15$ where $T_N = 0.080$ K as confirmed by a maximum in the *ac* susceptibility. For $x = 0.1$ we observe NFL behavior $C/T = a \ln(T/T_0)$ between 0.06 and ~2.5 K, i.e., over almost two decades in T, with $a = -0.578$ J/mol K^2 and $T_0 = 6.2$ K. T_0 corresponds exactly to $T_K = 6.2$ K of $CeCu_6$ [1,2] although this may be accidental. (The positive deviations above 2 K can be attributed to phonon and crystal-field contributions to C.) Concerning the critical

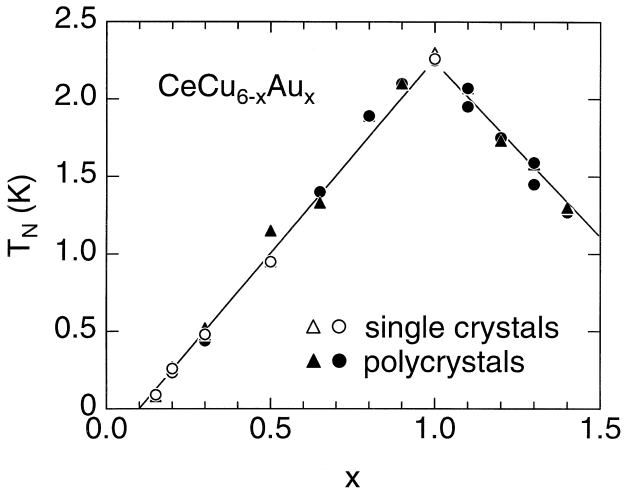

Fig. 1. Néel temperature T_N of $CeCu_{6-x}Au_x$ versus Au concentration x as determined from the specific heat (triangles) and magnetic susceptibility (circles) [27].

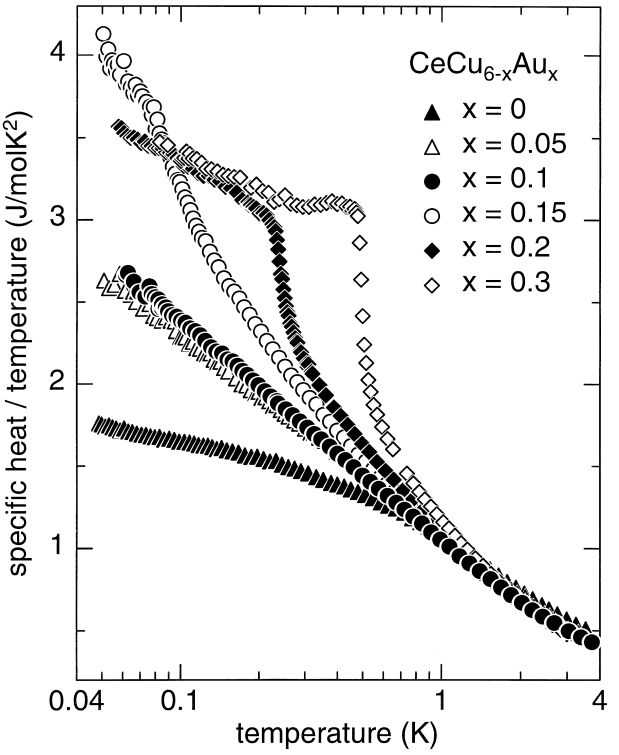

Fig. 2. Specific heat C of $CeCu_{6-x}Au_x$ plotted as C/T versus log T [31].

NFL behavior at x_c it is important to verify that it does not arise from some inhomogeneity of the alloys, i.e., a distribution of magnetic ordering temperatures. A recent μSR study has shown that there is no ordered magnetic moment in a $x = 0.1$ sample, with the detection limit $\mu < 10^{-3}\ \mu_B$ per Ce atom [32]. Likewise, a distribution of Kondo temperatures appears to be unlikely as an origin of NFL behavior [33].

As mentioned above, the onset of magnetic order in the $CeCu_{6-x}Au_x$ system is attributed to a weakening of J because of the increase of the molar volume upon alloying with Au. Indeed, T_N of $CeCu_{6-x}Au_x$ decreases roughly linearly under hydrostatic pressure p [34–36]. $T_N \approx 0$ is reached at 7–8 kbar for $x = 0.3$ [36] and at 3.2–4 kbar for 0.2 [36]. At these pressures both alloys exhibit NFL behavior in the specific heat, i.e., $C/T \sim -\ln T$, with, surprisingly, the same coefficients a and T_0 for both, and additionally for the NFL alloy with $x = 0.1$ and $p = 0$ [32]. On the other hand, application of $p = 6.0$ kbar for $x = 0.1$ drives this system towards FL behavior, as C/T at low T now falls even below the data of $CeCu_6$ for $p = 0$.

The transition to antiferromagnetic ordering appears in the magnetization $M(T)$ (measured in an applied field $B = 0.1$ T along the easy c direction) as a sharp maximum for $x = 0.3$ and as a kink in $M(T)$ for $x = 0.2$ [31]. For $x = 0.1$ the susceptibility exhibits a cusp for $T \to 0$ which can be modeled as $\chi \approx M/B \sim 1 - a\sqrt{T}$ between ~80 mK and 3 K (Fig. 3). Roughly the same T dependence of M/B is found upon reduction of the field to 0.01 T with a

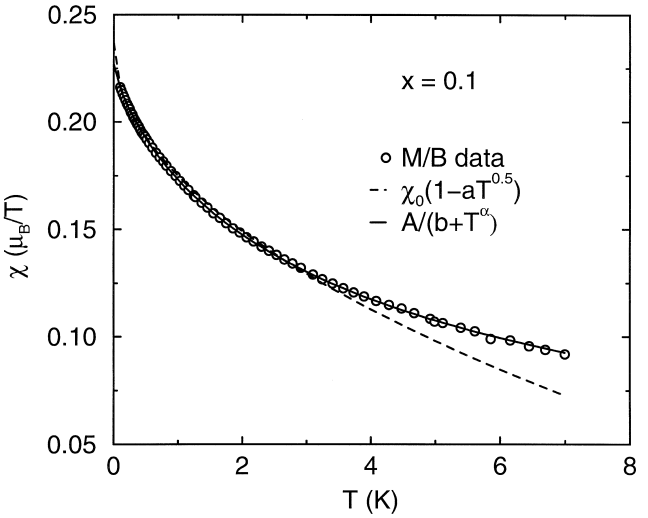

Fig. 3. Magnetic susceptibility $\chi \approx M/B$ of $CeCu_{5.9}Au_{0.1}$ (per Ce atom) as measured in an external magnetic field $B = 0.1$ T applied to the easy c direction versus temperature T [17]. Dashed line shows the temperature dependence $\chi \sim 1 - a\sqrt{T}$ [17] as obeyed up to 3 K, solid line the dependence $\chi = A/(b + T^{\alpha})$ with $\alpha = 0.8$, see also Eq. (3) below [38].

slightly stronger upturn towards low T below 0.3 K [37]. Motivated by inelastic neutron-scattering data (see below) Schröder et al. showed that the $\chi(T)$ data can be described very well by a different functional dependence, i.e., $\chi(T)^{-1} - \chi(0)^{-1} = aT^{\alpha}$ with $\alpha = 0.8$ [38]. This fit extends to 7 K, i.e., to well above T_K. This is surprising because the FL in $CeCu_6$ is formed only well below T_K.

Fig. 4 shows $\rho(T)$ for different $CeCu_{6-x}Au_x$ alloys for current parallel to the orthorhombic a direction. For $x < x_c \approx 0.1$, $\rho(T)$ increases at the lowest temperatures as $\rho(T) = \rho(0) + AT^2$ which is expected for a FL with dominant quasiparticle–quasiparticle scattering for $T \to 0$ as observed before for $CeCu_6$ [22]. For the magnetically ordered alloys with $0.15 \le x \le 0.3$, $\rho_a(T)$ and $\rho_c(T)$ (not shown) exhibit a kink a T_N and increase with decreasing $T < T_N$. These findings can be qualitatively interpreted in terms of the observed magnetic order: $\rho(T)$ increases below T_N for current directions with a non-zero projection of the magnetic ordering vector Q determined from the elastic neutron-scattering data discussed below [19]. An increase of $\rho(T)$ below T_N has been observed before in other HFS, for example, in $Ce_{1-x}La_xRu_2Si_2$ [39] and $CeRu_{2-x}Rh_xSi_2$ [40]. At $x_c = 0.1$, a T-linear resistivity signaling NFL behavior [17] is observed for all current directions [37].

The abundance of low-energy magnetic excitations when T_N is tuned to just zero, has been suggested early on to cause the NFL behavior at the magnetic instability [17]. However, the $-\ln T$ dependence of C/T and the linear T dependence of ρ in $CeCu_{6-x}Au_x$ at the magnetic instability have constituted a major puzzle ever since they were first reported because spin-fluctuation theories for 3D itinerant fermion systems predict [4,10] $C/T = \gamma_0 - \beta\sqrt{T}$ and $\Delta\rho \sim T^{3/2}$ for antiferromagnets ($z = 2$). In addition, T_N should depend on the control parameter $\delta_x = x - x_c$ or $\delta_p = p - p_c$ as $T \sim |\delta|^{\mu}$ with $\mu = z/(d + z - 2) = z/(z + 1)$ for $d = 3$ [4], while for $CeCu_{6-x}Au_x$ $\mu \approx 1$ for both δ_x and δ_p is found. In order to resolve this puzzle, neutron scattering was employed.

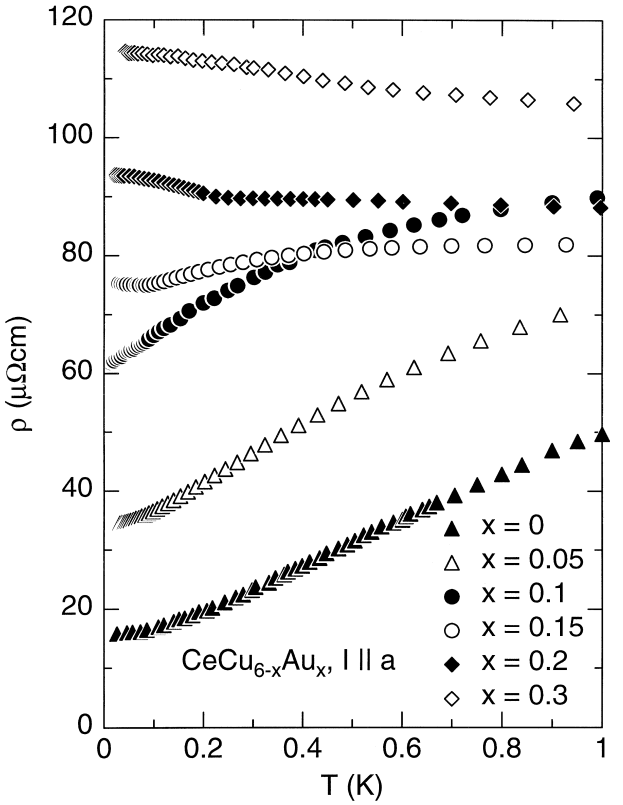

Fig. 4. Electrical resistivity ρ of $CeCu_{6-x}Au_x$ with the current I parallel to the a direction [37].

3. Magnetic structure and magnetic fluctuations in $CeCu_{6-x}Au_x$

The magnetic structure for $CeCu_{6-x}Au_x$ ($0.2 \le x \le 1$) was determined with elastic neutron scattering [19,41,42]. The magnetic ordering vector is $Q = (0.625\ 0\ 0.275)$ for $x = 0.2$ where the Bragg peaks are resolution limited (Fig. 5a), and remains almost constant up to $x = 0.4$ [42]. For larger x, Q jumps onto the a^* axis, $Q = (0.59\ 0\ 0)$ for $x = 0.5$. The positions of the Bragg peaks observed are displayed in Fig. 5b. Previously, short-range magnetic ordering had been found for $x = 0.2$ along the a^* axis [43]. This prompted Rosch et al. [11] to suggest an effectively 2D magnetic ordering on the basis that the broad feature observed along a^* exhibits a much smaller width along b^*. 2D critical fluctuations coupled to quasiparticles with 3D dynamics lead to the observed behavior $C/T \sim -\ln T$, $\Delta\rho \sim T$ and $T_N \sim |\delta|$, i.e., $\mu = 1$ [11].

A detailed investigation right at the critical concen-

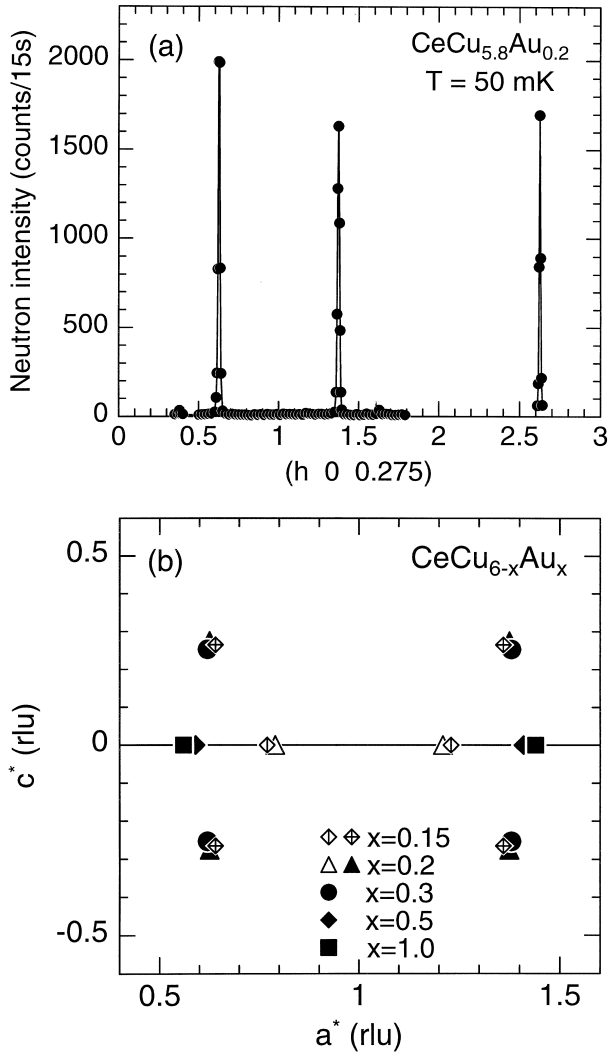

Fig. 5. (a) Resolution-limited magnetic Bragg reflections for $CeCu_{5.8}Au_{0.2}$ corresponding to a magnetic ordering vector $Q=(0.625\ 0\ 0.275)$ [19,45]. (b) Magnetic ordering vector Q for different x. Closed symbols denote long-range order, open symbols short-range order. Note the jump of Q to the a^* axis between $x=0.3$ and 0.5 [19,41,44,45].

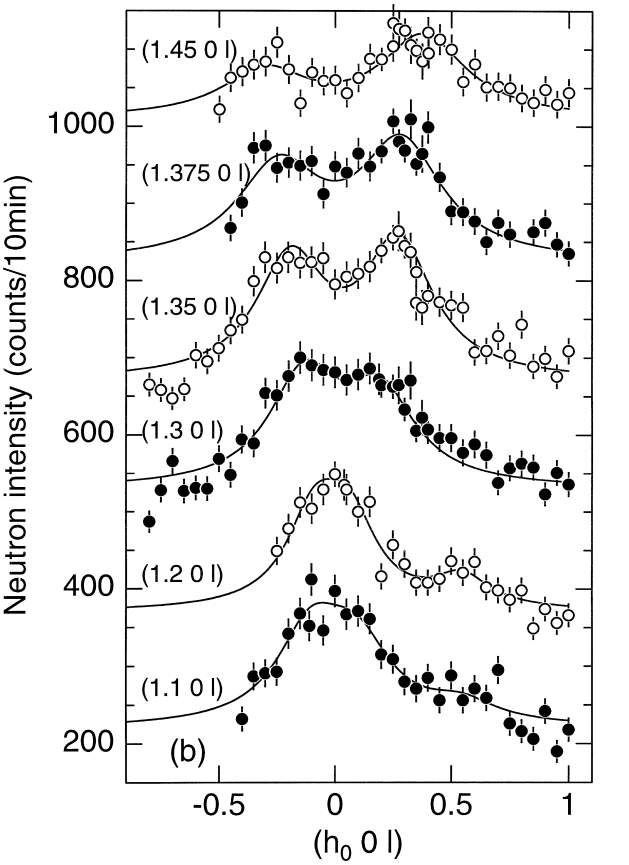

Fig. 6. Neutron-scattering intensity of $CeCu_{5.9}Au_{0.1}$ (energy transfer $\hbar\omega=0.1$ meV). Scans along l for different fixed h_0 in the a^*c^* plane at $T=70$ mK are shown. The scans are shifted by 150 counts/10 min with respect to each other [7]. Solid lines indicate Lorentzian fits with a width of (0.24 ± 0.2) Å^{-1} for all scans shown.

tration $x=0.1$ by Stockert et al. [44,45] showed that, as a matter of fact, the critical fluctuations as measured with an energy transfer of 0.10 meV are not confined to the a^* axis but extend into the a^*c^* plane. This is inferred from a large number of scans in the a^*c^* plane, some of which are shown in Fig. 6. Hence the dynamic structure factor $S(q, \hbar\omega=0.10\ \text{meV})$ has the form of rods (see Fig. 7). Yet, the main conclusion of the earlier work [11] remains valid, namely the presence of a quasi-1D dynamic feature in reciprocal space that corresponds to quasi-2D fluctuations in real space. The width of $S(q, \omega)$ perpendicular to the rods is roughly a factor of five smaller than along the rods. This is found for scans within the a^*c^* plane and also perpendicular to the a^*c^* plane, i.e., in the b^* direction [44]. It is interesting to note that the 3D ordering peaks for $x=0.2$ and 0.3 fall on the rods for $x=0.1$, which therefore can be viewed as a precursor of 3D ordering. From the width of the rods in reciprocal space, the prefactor of the logarithmic C/T dependence could be calculated to within a factor of two [44].

The spin fluctuations also develop a specific dynamic at $x=0.1$ [38]. The scattering function $S(q, E=\hbar w, T)$ or the susceptibility $\chi''=S\cdot(1-\exp(-E/k_BT))$ exhibit E/T scaling in the critical q region (e.g., at $Q_c=(0.8\ 0\ 0)$) which can be expressed by

$$\chi''(Q_c, E, T)=T^{-\alpha}g(E/k_BT) \quad (1)$$

with $\alpha=0.75$ [38], see Fig. 8. This demonstrates that the characteristic energy scale of the correlated fluctuations at this QPT is nothing else but k_BT. The exponent $\alpha\neq1$ indicates that the fluctuations do not have a Lorentzian lineshape. It does not change for other q away from the critical region. For all q the susceptibility can be expressed as

$$\chi^{-1}(q, E, T)=c^{-1}(f(q)+(-iE+aT)^{\alpha}). \quad (2)$$

This is strongly supported by the T dependence of the static uniform susceptibility $\chi(q=0, E=0)=M/B$

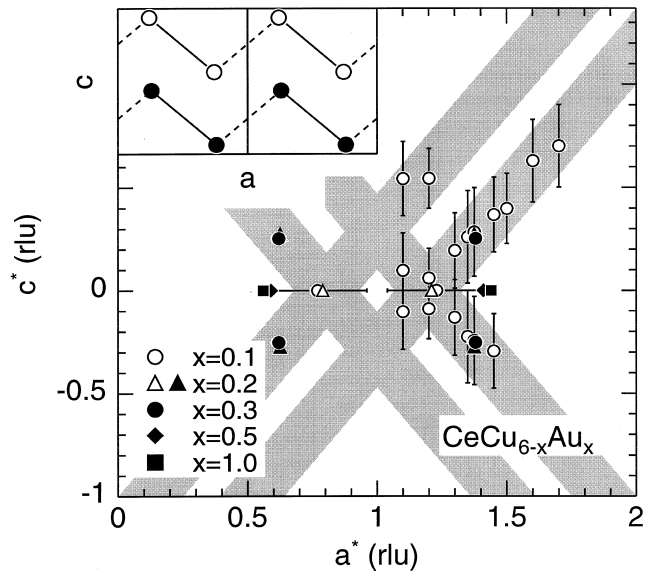

Fig. 7. Position of the dynamic correlations ($x = 0.1$, $\hbar\omega = 0.1$ meV, $T < 100$ mK) and magnetic Bragg peaks ($0.2 \le x \le 1.0$) in the a^*c^* plane in $CeCu_{6-x}Au_x$. Closed symbols for $x = 0.2$ represent short-range order peaks. The vertical and horizontal bars indicate the Lorentzian linewidths for $x = 0.1$. The four shaded rods are related by the orthorhombic symmetry (we ignore the small monoclinic distortion). The inset shows a schematic projection of the $CeCu_{6-x}Au_x$ structure in real space onto the *ac* plane where only the Ce atoms are shown. The rods in reciprocal space correspond to correlated planes in real space spanned by *b* and the lines in the inset [44,45].

$$\chi^{-1}(T) - \chi^{-1}(0) = c^{-1}aT^{\alpha} \tag{3}$$

with the same exponent $\alpha \approx 0.8$, see Fig. 3 above. The simple form of Eq. (2) separates static spatial correlations from the specific temporal correlations independent of q, thus demonstrating that these local fluctuations at the quantum critical point show a significant departure from Fermi-liquid behavior. Putting this scenario into a QPT framework with the only parameters d and z, consistency with C can be shown by modeling $f(q)$ by q^2 perpendicular to the rod structure and by a vanishing q^2 term but a finite q^4 term parallel to the rods. This leads to $z = 2.5$ and $d_{\rm eff} = 2.5$, thus obeying the condition $d = z$ for a vanishing power in C/T.

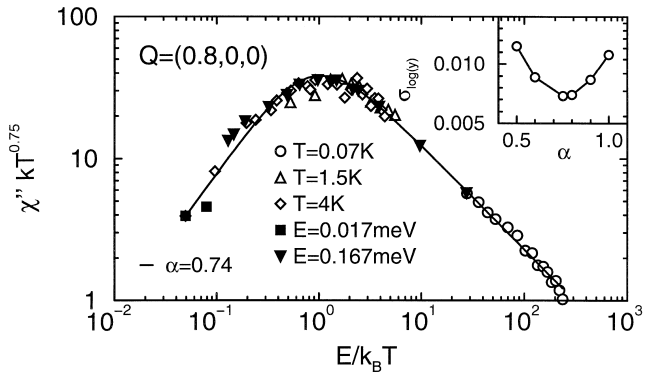

Fig. 8. Scaling plot of inelastic neutron-scattering data at $q = (0.8\ 0\ 0)$ for $CeCu_{5.9}Au_{0.1}$ versus E/k_BT. The inset shows deviations from the mean value per E/k_BT interval to check the quality of the scaling collapse with varying α. Solid line in the main part corresponds to a fit derived from Eq. (2) with $\alpha = 0.74$ [38] and $f(q) = 0$.

While the two neutron-scattering data sets for $x = 0.1$ [38,44] are not contradictory, the two interpretations lead to different predictions, depending on how the T dependence of the weakly correlated fluctuations along the rod direction is treated. The difference between absence of a temperature dependence or the presence of a weak T dependence, yielding $d = 2$ or $d_{\rm eff} = 2.5$, respectively, cannot be distinguished by the present data sets. However, one essential ingredient in both models is the unusual low effective dimension for the critical fluctuations in this material. A further point is that it is not easy to see where an effective 2D fluctuation spectrum originates from. The 2D planes are spanned by the *b* axis and the connection between next-nearest neighbor Ce atoms (see inset of Fig. 7). Only a microscopic model can establish if, perhaps, the low dimensionality arises from a strong anisotropy of the Fermi surface, the RKKY interaction, conduction-electron − local-moment hybridization, or a combination of these effects.

Despite these open questions it should be stressed that $CeCu_{6-x}Au_x$ is one of the best characterized HFS exhibiting NFL behavior. It is rewarding that the unusual behavior of the thermodynamic and transport properties at the QPT can be traced back to an unusual low-dimensional fluctuation spectrum determined by inelastic neutron scattering.

We now briefly discuss the behavior in an applied magnetic field B. In large fields, FL behavior is recovered for $x = 0.1$ [17]. One might ask if NFL behavior might arise at a magnetic field-induced instability in $CeCu_{6-x}Au_x$ for $x > 0.1$. In the light of the preceding discussion, however, it would be astonishing if an applied magnetic field B along c induces low-lying 2D spin excitations. Indeed, in $CeCu_{5.8}Au_{0.2}$ ($T_N = 0.25$ K) where the critical field is $B_c = 0.40$ T for $T \to 0$. $C/T \sim -\ln T$ is never observed at any field at/or beyond B_c [31]. Preliminary measurements of the (2.625 0 0.275) reflection show that its intensity decreases linearly with B and vanishes around 0.45 T for $T = 50$ mK [45]. The width along both a^* and c^* increase in a similar fashion with B, in contrast to the T dependence of the dynamic fluctuations at the critical concentration.

Recently, an apparent inducement of NFL behavior in a polycrystalline $CeCu_{4.8}Ag_{1.2}$ alloy by a magnetic field was reported, i.e., approximately $C/T \sim -\ln(T/T_0)$ between 0.35 and 2.5 K [46]. Subsequently, the same group reported specific-heat data down to 0.07 K on a $CeCu_{5.2}Ag_{0.8}$ single crystal with $T_N = 0.7$ K [47]. At a critical magnetic field $B_c = 2.3$ T applied to the easy direction, C/T varies logarithmically between ~ 1.5 and 0.2 K and then levels off towards lower T. Also, the resistivity exhibits a $T^{1.5}$ dependence at B_c. The authors

interpret the data within the conventional spin-fluctuation scenario, with $d = 3$ and $z = 2$. However, this model [4,10] was developed for spin fluctuations for $B = 0$. It will be interesting to compare the magnetic order and spin dynamics in $CeCu_{6-x}Ag_x$ with $CeCu_{6-x}Au_x$ in a magnetic field.

In an attempt to unify the NFL behavior in various systems, Kambe et al. [48,49] compared different HFS at the magnetic instability in terms of the SCR model. Because of the convincing experimental evidence of low-dimensional fluctuations in $CeCu_{6-x}Au_x$, this system should not, however, be pressed into the 3D category. A recent thorough inelastic neutron-scattering experiment on $Ce_{0.925}La_{0.075}Ru_2Si_2$, i.e., at the critical La concentration for the onset of magnetic order, showed 3D correlations for this system [50]. However, the linewidth Γ of the intersite dynamic fluctuations does not quite scale to zero as it should for a QPT. This might indicate that $x = 0.075$ is a little off the quantum critical point. The linewidth is reduced by a factor of 5, while the correlation length for $T \rightarrow 0$ is only 1.5 times larger than for pure $CeRu_2Si_2$. The dynamic susceptibility $\chi(q,\omega)$ is interpreted in terms of the random phase approximation which yields an overall satisfactory agreement between the parameters of the SCR model as derived from inelastic neutron scattering and those derived from the specific heat, although Γ as determined by the two methods differs by a factor of two [50].

4. Orthorhombic–monoclinic phase transition in $CeCu_{6-x}Au_x$

$CeCu_6$ undergoes a structural phase transition at $T_{om} \approx 220$ K from a high-T orthorhombic (Pnma) to a low-T monoclinic ($P2_1/c$) structure [51,52], with a monoclinic angle of $\beta \approx 91.5°$. Since it had been known for some time that $CeCu_{5.5}Au_{0.5}$ exhibits the orthorhombic structure down to 50 mK [41], a systematic investigation appeared to be necessary in order to look for a possible influence of the structural phase transition on NFL properties. Experiments were carried out at the powder diffractometer D2B at the ILL for $x = 0$ and 0.1. The Rietveld method was used to determine the lattice constants and β. Fig. 9a shows the square of the distortion ($ac \cos \beta$) playing the role of the order parameter, as a function of T. The linear dependence of $(ac \cos \beta)^2$ on T shows that the critical exponent for the order parameter assumes the mean-field value 1/2, in agreement with earlier studies [51]. We obtain $T_{om} = 237$ K for $x = 0$ and 71 K for $x = 0.1$. The latter value is in agreement with that derived from ultrasonic measurements [53]. The monoclinic angles are determined to $\beta = 91.42°$ for $x = 0$ and 90.72° for $x = 0.1$, both at 1.5 K. For $x = 0.15$ no indication of a monoclinic distortion was found down to 1.5 K.

Fig. 9b shows that $T_{om}(x)$ as determined from neutron scattering and additional X-ray scattering experiments depends linearly on x, suggesting a critical concentration $x \approx 0.14$ where T_{om} vanishes. The strong suppression of T_{om} upon Au doping can be simply understood as follows. The monoclinic distortion decreases the volume of the coordination polyhedron of the Cu(2) site in $CeCu_6$ [51,54]. This site has the largest coordination polyhedron of the five inequivalent Cu sites and consequently is occupied by the larger Au atom up to $x = 1$, thereby reducing the excess volume. This argument is supported by recent experiments of the thermal expansion which show that T_{mo} decreases under pressure which likewise reduces the excess volume [55].

The suppression of the monoclinic transition upon Au doping occurs in roughly the same concentration range as the onset of NFL behavior at the verge of long-range magnetic order. However, there seems to be no direct connection between both phenomena because (i) for $x = 0.1$, T_{om} is still at rather elevated temperatures compared to

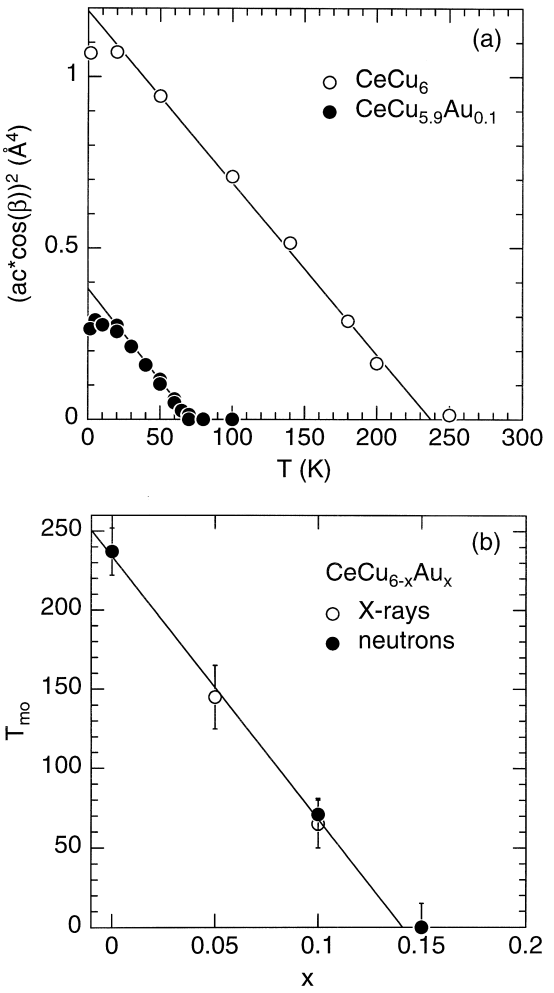

Fig. 9. (a) Square of the monoclinic distortion $(ac \cos \beta)^2$ for $CeCu_{6-x}Au_x$. Solid lines indicate a linear fit to the data. (b) Dependence of the transition temperature T_{om} on x as determined by neutron (closed symbols) and X-ray diffraction (open symbols).

the low-T NFL behavior, and (ii), even more importantly, NFL behavior for higher concentration without monoclinic transition ($x = 0.2$ and $x = 0.3$) is induced by pressure which on the other hand suppresses the monoclinic transition where present for lower x and therefore stabilizes the orthorhombic structure.

5. Conclusions

$CeCu_{6-x}Au_x$ is one of the best characterized systems displaying the full fledged competition between Kondo effect leading to local singlets and RKKY interaction leading to long-range magnetic order. The incommensurate antiferromagnetic order observed for $x > 0.1$ has been investigated in detail by elastic neutron scattering. An unexpected feature is the jump of the magnetic ordering vector occurring between $x = 0.3$ and 0.5. The anomalous behavior of the thermodynamic and transport properties of $CeCu_{6-x}Au_x$ at the quantum critical point $x = 0.1$ between nonmagnetic and magnetically ordered groundstates has been shown to arise from magnetic fluctuations with an effective dimension smaller than three. While the dynamic fluctuations measured at fixed energy transfer have a pronounced q dependence with a strong anisotropy, unexpected for a precursor of three-dimensional magnetic ordering, the dynamic susceptibility is determined by unusual temporal fluctuations that are independent of q, i.e., local in character. This sheds new light on the interplay between long-range magnetic correlations and local dynamics at the quantum critical point. Further neutron-scattering experiments are necessary to corroborate these findings. Finally, we have shown that the weak orthorhombic–monoclinic distortion occurring in $CeCu_6$ below ~ 220 K is quickly suppressed with increasing x and is unrelated to the quantum critical phenomena discussed. It is hoped that the present thorough neutron-scattering study of $CeCu_{6-x}Au_x$ will be followed by investigations on other rare-earth systems that are close to a magnetic–nonmagnetic quantum phase transition.

Acknowledgements

The results presented in the review have grown out of a fruitful collaboration with many colleagues and students. We would like to thank in particular our colleagues G. Aeppli, T. Chattopadhyay, P. Coleman, M. Loewenhaupt, N. Pyka and A. Rosch. Neutron scattering experiments have been carried out at the Institut Laue-Langevin Grenoble, the Risø National Laboratory and the Hahn-Meitner-Institut Berlin. We are grateful to these institutions and their staff for the possibility to perform these experiments. We would like to acknowledge the support provided by the European Science Foundation within the program on Fermi-liquid instabilities in correlated metals (FERLIN) and by the Deutsche Forschungsgemeinschaft.

References

[1] P. Fulde et al., in: H. Ehrenreich, D. Turnbull (Eds.), Solid State Physics, Vol. 41, Academic Press, San Diego, CA, 1988, p. 1.
[2] N. Grewe, F. Steglich, in: K.A. GschneidnerJr., L. Eyring (Eds.), Handbook on the Physics and Chemistry of Rare Earths, Vol. 14, Elsevier, Amsterdam, 1991, p. 343.
[3] J.A. Hertz, Phys. Rev. B 14 (1976) 1165.
[4] A.J. Millis, Phys. Rev. B 48 (1993) 7183.
[5] Proceedings of the Conference on Non-Fermi liquid behavior in Metals, Santa Barbara 1996, published as a special issue of J. Phys.: Cond. Matt. 8 (1996) 9675–10148.
[6] Z. Fisk et al., Jpn. J. Appl. Phys. Suppl. 3 (26) (1987) 1882.
[7] K. Kadowaki, S.B. Woods, Solid State Commun. 58 (1986) 507.
[8] S. Doniach, Physica B 91 (1977) 213.
[9] P. Thalmeier, B. Lüthi, in: K.A. GschneidnerJr., L. Eyring (Eds.), Handbook on the Physics and Chemistry of Rare Earths, Vol. 14, Elsevier, Amsterdam, 1991, p. 225.
[10] T. Moriya, T. Takimoto, J. Phys. Soc. Jpn. 64 (1995) 960, and Refs. therein.
[11] A. Rosch et al., Phys. Rev. Lett. 79 (1997) 159.
[12] O.O. Bernal et al., Phys. Rev. Lett. 75 (1995) 2023.
[13] E. Miranda et al., J. Phys.: Cond. Matt. 8 (1996) 9871.
[14] A.H. Castro Neto et al., Phys. Rev. Lett. 81 (1998) 3531.
[15] R.B. Griffiths, Phys. Rev. Lett. 23 (1969) 17.
[16] M.C. de Andrade et al., Phys. Rev. Lett. 81 (1998) 5620.
[17] H.v. Löhneysen et al., Phys. Rev. Lett. 72 (1994) 3263.
[18] H.v. Löhneysen, J. Phys.: Cond. Mater. 8 (1996) 9689.
[19] H.v. Löhneysen et al., Eur. J. Phys. B 5 (1998) 447, and Refs. therein.
[20] H.v. Löhneysen, J. Magn. Magn. Mater. 200 (1999) 532.
[21] Y. Onuki, T. Komatsubara, J. Magn. Magn. Mater. 63/64 (1987) 281.
[22] A. Amato et al., J. Low Temp. Phys. 68 (1987) 371.
[23] E.A. Schuberth et al., Phys. Rev. B. 51 (1995) 12892.
[24] L. Pollack et al., Phys. Rev. B 52 (1995) R15707.
[25] J. Rossat-Mignod et al., J. Magn. Magn. Mater. 76/77 (1988) 376.
[26] H.v. Löhneysen et al., Physica B 186–188 (1993) 590.
[27] T. Pietrus et al., Physica B 206/207 (1995) 317.
[28] A. Germann et al., J. Phys. Coll. 49 (1988) C8–755.
[29] M.R. Lees, B.R. Coles, J. Magn. Magn. Mater. 76/77 (1988) 173.
[30] C. Paschke et al., J. Low Temp. Phys. 97 (1994) 229.
[31] H.v. Löhneysen et al., Physica B 223/224 (1996) 471.
[32] A. Amato et al., Phys. Rev. B 52 (1995) 54.
[33] O.O. Bernal et al., Phys. Rev. B 54 (1996) 13000.
[34] A. Germann, H.v. Löhneysen, Europhys. Lett. 9 (1989) 367.
[35] B. Bogenberger, H.v. Löhneysen, Phys. Rev. Lett. 74 (1995) 1016.
[36] M. Sieck et al., Physica B 230–232 (1997) 583.
[37] H.v. Löhneysen et al., J. Magn. Magn. Mater. 177–181 (1998) 12.
[38] A. Schröder et al., Phys. Rev. Lett. 80 (1998) 5623.
[39] R. Djerbi et al., J. Magn. Magn. Mater. 76/77 (1988) 260.
[40] Y. Miyako et al., Physica B 230–232 (1997) 1011.
[41] A. Schröder et al., Physica B 199/200 (1994) 47.
[42] H. Okumura et al., J. Magn. Magn. Mater. 177–181 (1998) 405.
[43] O. Stockert et al., Physica B 230–232 (1997) 247.
[44] O. Stockert et al., Phys. Rev. Lett. 80 (1998) 5627.
[45] O. Stockert, Dissertation, Universität Karlsruhe, 1999.
[46] K. Heuser et al., Phys. Rev. B 57 (1998) R4198.
[47] E.-W. Scheidt et al., Phys. Rev. B 98 (1998) R 15959.

[48] S. Kambe et al., J. Phys. Soc. Jpn. 65 (1996) 3294.
[49] S. Kambe et al., J. Low Temp. Phys. 108 (1997) 383.
[50] S. Raymond et al., J. Low Temp. Phys. 109 (1997) 205.
[51] M.L. Vrtis et al., Physica B 136 (1986) 489.
[52] E. Gratz et al., J. Magn. Magn. Mater. 63/64 (1987) 312.
[53] D. Finsterbusch et al., Ann. Phys. (Leipzig) 5 (1996) 184.
[54] H. Asano et al., J. Phys. Soc. Jpn. 55 (1986) 454.
[55] K. Grube et al., Phys. Rev. B 60 (1999) 11947.